Journal of Animal Environment

(E-ISSN 2717-1396, ISSN 2717-1388)

From Agricultural Residue to Nanomaterial: Extraction and Characterization of Cellulose Nanocrystals from Pigeon Pea Husk (*Cajanus cajan*)

Alka Nanda[1], Neetu Singh[1]*, Ayushi Singh[1], Tanya Singh[1], Puja Kumari[1], Prashant Pandey[2]

[1]Department of Food and Nutrition, School of Home Science, Babasaheb Bhimrao Ambedkar University, Lucknow, Uttar Pradesh-226025

[2]Department of Pharmaceutical Sciences, Babasaheb Bhimrao Ambedkar University, Lucknow, Uttar Pradesh-226025

***Correspondence**

Prof. Neetu Singh

Department of Food and Nutrition, School of Home Science

Babasaheb Bhimrao Ambedkar University, Lucknow, Uttar Pradesh

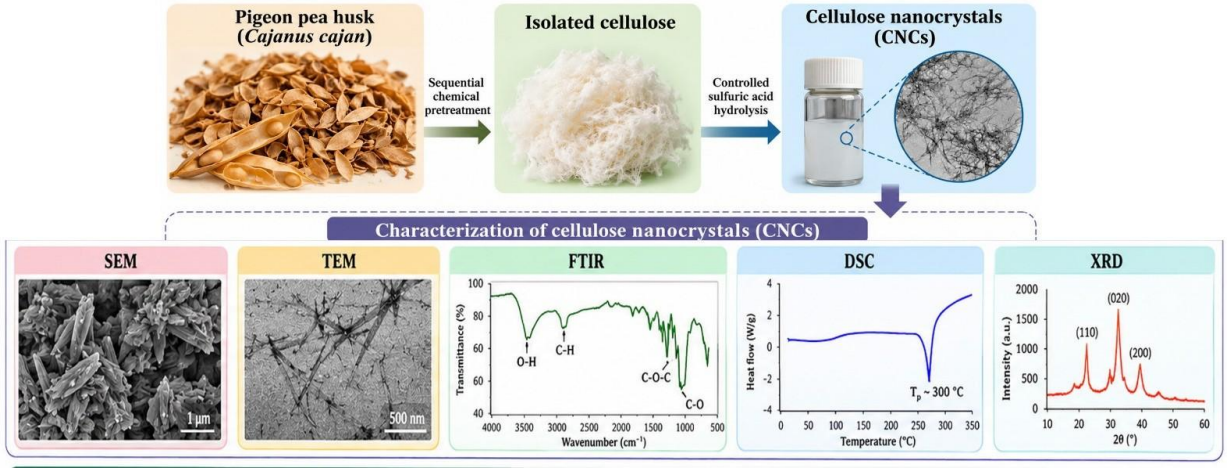
Email: neetubbau@gmail.com

Abstract

Cellulose nanocrystals (CNCs) were produced from pigeon pea husk (*Cajanus cajan*), an underutilized agro-industrial residue, through controlled sulfuric acid (H_2SO_4) hydrolysis. Hydrolysis with 64 wt.% H_2SO_4 at 45 °C for half an hour, followed by dialysis, probe sonication, and freeze-drying, yielded 61.25% CNCs relative to purified cellulose. Scanning and transmission electron microscopy (SEM & TEM) confirmed rod-shaped nanocrystals with a mean length of 335 ± 12.91 nm, width of 28.80 ± 2.67 nm, and aspect ratio of 11.63. X-ray diffraction (XRD) analysis showed a crystallinity index of 91.83%, indicating a highly crystalline structure. Dynamic light scattering (DLS) measurements showed a hydrodynamic diameter of 288.08 ± 9.07 nm and a polydispersity index (PDI) of 0.451, while the zeta potential of −43.21 ± 2.34 mV indicated favourable electrostatic characteristics for aqueous dispersion. Fourier-transform infrared (FTIR) spectroscopy confirmed the characteristic cellulose functional groups, while differential scanning calorimetry revealed a prominent thermal event near 300 °C. These findings highlight pigeon pea husk as a sustainable, renewable precursor for cellulose nanocrystal (CNC) production and demonstrate the potential of agricultural residues as valuable feedstocks for advanced nanocellulose materials. The physicochemical and structural characteristics of the extracted CNCs provide a basis for further research into their material performance and potential applications in nanocomposites, functional materials, and sustainable material development.

Keywords: Pigeon pea husk, *Cajanus cajan*; agricultural residue valorization; acid hydrolysis; cellulose nanocrystals

Graphical Abstract



1. Introduction

Cellulose derived nanomaterials are of growing interest due to the rise in demand for sustainable

***Corresponding Author:**
Received: 25th May, 2026; Revised: 6th July, 2026; Accepted: 28th July, 2026; Available Online: 29th August, 2026
(DOI): 10.70102/AEJ.2026.18.8s.32

biomaterials. Cellulose is one of the most prevalent renewable polysaccharides and a potential precursor of cellulose nanocrystals (CNCs) with high crystallinity, nanoscale dimensions, low density and mechanical stability. Their properties are affected by the source of cellulose, the lignocellulosic content, the pretreatment and extraction conditions [1-3].
Lignocellulosic biomass contains cellulose, hemicellulose, lignin, extractives, proteins, and inorganic constituents, whose complex association complicates cellulose purification and nanocrystal isolation. Nanocellulose extraction methods include physical methods such as high-pressure homogenization, grinding, ultrasonication and blending; chemical procedures such as H_2SO_4 or hydrochloric acid (HCl) hydrolysis and TEMPO-mediated oxidation; and enzyme-assisted hydrolysis [4-8]. These physical methods can be used alone or in combination in order to improve the extraction efficiency and adjust the physicochemical characteristics of the nanomaterials [9, 10].

The most common method for obtaining CNCs from lignocellulosic material is sequential chemical pretreatment and controlled acid hydrolysis. Pretreatment removes extractives, lignin, hemicellulose, and other non-cellulosic constituents, while acid hydrolysis preferentially cleaves glycosidic linkages in less-ordered cellulose regions, releasing crystalline domains. Sulfuric acid hydrolysis also introduces surface sulfate ester groups that influence CNC surface charge and colloidal stability. However, excessive acid concentration or prolonged hydrolysis may degrade cellulose and reduce yield, highlighting the importance of optimizing processing conditions to balance purification, recovery, structural integrity, and surface properties [6, 7, 11].

Cellulose and CNCs have been isolated from several agricultural residues, including rice straw [12-14], wheat straw [15], oat straw, barley straw and associated husks [13, 16, 17], rice husk [18, 19], sorghum straw, corn straw [20], and soybean straw [21, 22]. These studies reveal the feasibility of agricultural by-products as an alternative feedstock for cellulose-based nanomaterials. Nevertheless, differences in botanical origin, cell-wall architecture, chemical composition, and pretreatment requirements can substantially influence the efficiency of cellulose isolation and the qualities of the resultant CNCs [3]. In particular, the presence of lignin, hemicellulose, proteins, and phenolic constituents may complicate the purification of cellulose from leguminous biomass. A systematic investigation of such feedstocks is therefore necessary to establish effective extraction strategies and clarify the relationships between biomass composition, processing conditions, and the structural properties of the recovered nanocrystals.

Pigeon pea (*Cajanus cajan* (L.) Millsp.), a crucial pulse crop cultivated across Asia, Africa, and South America, is widely consumed as dhal, particularly in India. Dehulling generates substantial by-products, with husk and other residual fractions accounting for approximately 25–35% of the processed material [23-27]. These residues are often discarded or used as an undervalued livestock feed, highlighting their potential for conversion into value-added biomaterials.

Pigeon pea husk (PPH), a lignocellulosic residue, was subjected to sequential dewaxing, acidified sodium chlorite bleaching, and alkaline treatment for isolation of cellulose, followed by controlled H_2SO_4 hydrolysis to produce cellulose nanocrystals (CNCs). The study hypothesized that sequential pretreatment and optimized hydrolysis would facilitate non-cellulosic component removal and isolate crystalline domains with distinct physicochemical properties. Cellulose recovery was $59.7 \pm 1.4\%$ of the initial dry PPH. Accordingly, the study aimed to isolate cellulose from PPH, optimize CNC production, and characterize the resulting materials using TEM, SEM, Particle size and zeta potential measurements using dynamic light scattering (DLS), FTIR, XRD and DSC. The findings may provide a basis for future investigations into CNC incorporation in biodegradable food-packaging materials and pharmaceutical biomaterials; however, these applications were outside the scope of the present investigation.

2. Materials and Methods

2.1 Materials

Pigeon pea husk (PPH), a by-product of pigeon pea processing, was procured from a local mill in Aliganj, Lucknow, Uttar Pradesh, India. Toluene (C_7H_8, 99.5%, AR/ACS grade) and ethanol (C_2H_5OH, 99.9% purity) were used for dewaxing the raw biomass. Sodium chlorite ($NaClO_2$, 80%, flakes, LR grade) and glacial acetic acid (CH_3COOH, 99.7%, ACS/GR grade; EMD) were used for the delignification and bleaching treatment. Potassium hydroxide (KOH, 85%, AR/BP/USP grade) was employed for alkaline treatment during cellulose isolation, while sulfuric acid (H_2SO_4, 98%, AR grade) was used for the controlled acid hydrolysis of purified cellulose to obtain cellulose nanocrystals (CNCs). All compounds were utilized without further purification. Double-distilled water was obtained using a laboratory double-distillation apparatus and used throughout the experimental procedures. All analytical-grade reagents were procured from SRL Pvt. Ltd., Mumbai, India, unless otherwise specified.

2.2 Pigeon pea husk powder preparation

Pigeon pea husk was soaked in water for 20 min, washed twice with tap water, and oven-dried at 60 °C for 6 h. The dried husk was ground using a laboratory blender (Sumeet Research and Holdings Limited, Chennai, India) and sieved through a 300 µm sieve to obtain a homogeneous powder.

2.3 Isolation of cellulose from pigeon pea husk

Dried pigeon pea husk (PPH) powder was used for cellulose isolation following reported methods [12, 13, 28, 29] with some alterations. Briefly, 30 g of powder was dewaxed using 450 mL of toluene–ethanol (2:1, v/v) at room temperature for 20 h, filtered through Whatman No. 41 filter paper, washed with ethanol, and dried at 55 °C for 24 h. The dewaxed powder was treated with 1000 mL of 1.4% (w/v) acidified sodium chlorite ($NaClO_2$), adjusted to pH 3.0–4.0 using 5% acetic acid, at 70 °C for 5 h to remove lignin. The reaction was quenched with ice, and the residue was washed with distilled water until neutral and dried at 70 °C to obtain holocellulose.

The dehydrated holocellulose was suspended in 600 mL of 5% potassium hydroxide (KOH), agitated at ambient temperature for 24 hours, and subsequently heated to 90 °C for 2 hours. The suspension was centrifuged at 4000 rpm for 20 min, and the recovered cellulose was washed until neutral and dried at 105 °C to obtain α-cellulose.

Lignin and hemicellulose-associated fractions were estimated from sequential gravimetric mass changes during chemical treatment. As standardized compositional analysis was not performed, these values represent operational estimates that may also include mass losses from other soluble or degraded constituents. Protein removal was not independently quantified. Cellulose recovery was calculated using Equation (1):

$$\text{Cellulose recovery (\%)} = \frac{mass\ of\ purified\ cellulose\ recovered}{initial\ dry\ mass\ of\ PPH} \times 100 \quad (1)$$

All extraction experiments were performed using three independent batches, each starting with 30 g of dried pigeon pea husk (PPH). Cellulose recovery values are reported as the mean ± standard deviation calculated from three independent extraction batches (n = 3).

2.4 Preparation of CNCs

CNCs were extracted from cellulose isolated from PPH by sulfuric acid hydrolysis, following previously reported methods with minor modifications [12, 13]. Briefly, the cellulose was treated with 64 wt.% sulfuric acid at an acid-to-cellulose ratio of 8.75 mL/g and maintained at 45 °C for 30 min, based on established protocols for softwood pulp and rice straw [12, 30, 31]. The hydrolysis reaction was halted by introducing tenfold the reaction volume of ice-cold distilled water.

The resulting suspension was subjected to centrifugation at 5000 rpm for 25 min at 10 °C. The collected material was subsequently dialyzed against distilled water using regenerated seamless cellulose dialysis tubing with a molecular weight cut-off of 12,000–14,000 Da (HiMedia Laboratories Pvt. Ltd., Mumbai, India). Distilled water was obtained using a LabQuest Borosil SDU150 single-distillation unit. Following dialysis, the suspension pH was adjusted to 7.0 using 5% sodium hydroxide (NaOH) solution.

To reduce particle agglomeration, the CNC suspension underwent sonication for 10 min with a PRO650 probe sonicator (Model V20160303, Labman Scientific Instruments Pvt. Ltd., Chennai, India) at 40% power, with alternating 2 s on and 2 s off pulses. Sonication was performed in a plastic beaker immersed in an ice-water bath to prevent overheating. The resulting suspension was frozen for 24 h and subsequently freeze-dried at 45 °C for 50 h using a lyophilizer (M/S Operon, South Korea). The dried CNCs were stored in airtight, dark-colored glass bottles until further characterization.

The CNC yield was determined (using Eq. 2) following [32].

$$\text{CNC Yield (\%)} = \frac{Mass\ of\ dried\ CNC's}{Initial\ mass\ of\ cellulose} \times 100 \quad (2)$$

The extraction procedure was performed using three independently prepared batches, and the CNC yield was calculated for each batch. The outcomes are presented as mean ± standard deviation (n = 3).

2.5 Characterization of CNC

2.5.1 Morphological analysis

2.5.1.1 Transmission electron microscopy (TEM) analysis

The morphology of CNCs derived from pigeon pea husk was investigated using transmission electron microscopy (TEM; JEM-2100F, JEOL Ltd., Tokyo, Japan) operated at 200 kV. TEM analyses were conducted in duplicate. Prior to imaging, the sample was diluted to 0.2 wt% and probe-sonicated to obtain well-dispersed, aggregate-free suspension. Each suspension then was placed on 10 µL carbon coated copper TEM grids with a Labnet micropipette. The prepared grids were air-dried, and micro-graphs were taken at desired magnifications to evaluate the characteristics of particle dispersion and the morphology of the particles [12, 33, 34].

2.5.1.2 Scanning electron microscopy (SEM) analysis

The surface morphology and microstructural features of pigeon pea husk-derived CNCs were analyzed using a scanning electron microscope (JSM-6490LV, JEOL, Japan) operated at an accelerating voltage of 15 kV and a current of 58 µA [12, 34].

The CNC suspension (0.2 wt.%) was prepared for SEM analysis by drop-casting onto aluminum foil. The sample was examined using a scanning electron microscope to determine the morphology, particle dispersion, and structural characteristics of the CNCs. All analyses were performed in triplicate [35, 36].

The diameter and size distribution of CNCs were further determined by analyzing approximately 150 representative particles from the acquired electron micrographs using ImageJ software (Version 1.53k, National Institutes of Health, Bethesda, MD, USA).

2.5.2 Particle size and zeta potential measurements using dynamic light scattering (DLS)

The hydrodynamic particle size, polydispersity index (PDI), and zeta potential of pigeon pea husk-derived cellulose nanocrystals (CNCs) were measured using a ZTS1240 Zetasizer (Malvern Panalytical, UK) equipped with a 633 nm He–Ne laser and a 173° backscatter detector. For particle size and PDI analysis, the 2% (w/v) CNC suspension was diluted to 0.5% (w/v) with deionized water and measured at 25 °C in a disposable cuvette. For zeta potential analysis, the suspension was diluted 1:1 (v/v) with distilled water and analyzed in folded capillary cells at 25 °C. Zeta potential was determined using electrophoretic mobility employing the Smoluchowski model. All measurements were conducted in triplicate, and outcomes were presented as average values [11].

2.5.3 Fourier transform infrared spectroscopy (FTIR) analysis

FTIR spectroscopy was employed to characterize the chemical structure and identify the functional groups present in the cellulose nanocrystals (CNCs). Spectral analysis was performed using a Thermo Nicolet 6700 spectrometer (Thermo Fisher Scientific, USA). Prior to analysis, each sample was thoroughly mixed with potassium bromide (KBr) in a sample-to-KBr weight ratio of 1:3 and compressed into transparent pellets. The FTIR spectra were obtained within a wavenumber range of 4000–500 cm^{-1}, utilizing 32 scans for each sample at a spectral resolution of 4 cm^{-1}. The acquired spectra were normalized and plotted using OriginPro 10.1.0.178 (64-bit) software (OriginLab Corporation, USA).

2.5.4 X-Ray diffraction (XRD) analysis

XRD analysis was conducted to assess the crystalline structure and crystallinity of cellulose nanocrystals (CNCs) isolated from pigeon pea husk. The analysis was conducted using an X-ray diffractometer (D8 Advance Eco, Bruker, Germany) equipped with Cu-Kα radiation (λ=1.542 A°), operated at a voltage of 30 kV and a current of 10 mA. The dried CNC sample was mounted on a quartz substrate, and the diffraction pattern was recorded over a 2θ range of 10–60° at a scanning speed of 2° min^{-1}. The obtained diffractogram was analyzed using TOPAS software, while OriginPro 10.1.0.178 (OriginLab Corporation, USA) was used for baseline correction and peak-profile analysis. The crystallinity index (C_i) was determined by estimating the crystalline (A_c) and amorphous (A_a) contributions from the corrected diffraction pattern, following the area-based method [11, 37] using Eq. (3):

$$C_i\,(\%) = \frac{Ac}{A_c + Aa} \times 100 \quad (3)$$

2.5.5 Differential Scanning Calorimetry (DSC)

DSC analysis was conducted to examine the thermal characteristics of cellulose nanocrystals (CNCs) using a DSC 25 instrument (TA Instruments, USA). An aluminum sample pan was used to accurately weigh and position approximately 0.01 g of oven-dried sample, whereas a vacant aluminum pan acted as the reference. All measurements were conducted under a nitrogen (N_2) atmosphere to minimize oxidative degradation during thermal analysis. The samples were initially equilibrated at 10 °C and subsequently heated to 350 °C at a constant heating rate of 10 °C min^{-1}. Heat flow was continuously recorded as a function of temperature to characterize the thermal transitions and assess changes in the thermal behaviour of the sample.

3 Results and discussion

3.1 Yield of Cellulose and Cellulose Nanocrystals (CNC) from pigeon pea husk

The dried pigeon pea husk powder was characterized for its lignocellulosic composition by sequential solvent extraction, delignification, and alkali treatment. The raw biomass was determined to contain 59.7±1.4% cellulose, 14.04±2.7% hemicellulose, 23.08±1.6% lignin, and 3.17±1.5% extractives, based on the dry-weight mass balance achieved at each stage of the extraction protocol. The considerable amount of cellulose (59.7%) found in pigeon pea husk was significantly higher compared to other agricultural residues like wheat straw (30–43.4%), rice husk (32.7–41.52%), corn husk (36%), wheat husk (34%), rice straw (36.2–47%), corn straw (51.53%), and pigeon pea pod waste (59.15%). These findings further support the

use of PPH as a valuable lignocellulosic source for cellulose extraction and CNC formation [14, 20, 38, 39].

The yield of CNCs obtained from pigeon pea husk under optimized hydrolysis conditions (64 wt.% sulfuric acid, cellulose-to-acid ratio of 1 g/8.75 mL, hydrolysis time of 30 min, and temperature of 45 °C) was determined to be 61.25±2.3%. The temperature of 45°C selected for acid hydrolysis is proven to be more controlled than those carried out at higher temperatures such as 65°C [12]. Cellulose hydrolysis with sulfuric acid yielded a relatively high CNC yield (≥50%) compared with previous studies [6, 12, 40, 41]. This difference in yield can be mainly attributed to hydrolysis parameters, because CNC recovery depends not only on the cellulose source but also on the acid concentration, cellulose-to-acid ratio, hydrolysis time, reaction temperature, and post-treatment, such as ultrasonication [13, 42]. The relatively high CNC yield obtained in the present study, can be attributed to the relatively mild hydrolysis conditions used for sulfuric acid treatment (45 °C, 30 min, 64 wt.% H_2SO_4). In such a case, the domains of amorphous cellulose may not have been fully degraded, which would reduce over-depolymerization of cellulose chains and the amount of fragmented cellulose that would enter the soluble phase. However, there might be partial retention of less-ordered cellulose regions, which contributed to the improved recovery yield. In addition, the following probe sonication treatment may have provided additional dispersion and stabilization of nanocrystalline particles, reducing the aggregation of particles and minimizing the material lost during the centrifugation and washing procedures, which may be further contributing to the increased CNC recovery.

3.2 Morphological analysis

3.2.1 TEM

TEM micrographs (Fig. 1a) revealed distinct rod-shaped cellulose nanocrystals (CNCs) derived from pigeon pea husk, confirming the formation of nanoscale crystalline structures following controlled sulfuric acid hydrolysis. The nanocrystals exhibited a tendency to form aggregates, potentially due to intermolecular hydrogen bonding and the high surface energy of cellulose nanomaterials, which may complicate dimensional analysis. Similar rod-like morphologies have been reported for CNCs derived from *Cucumis sativus* and oil palm trunk biomass [11, 43]. Hydrolysis of less-ordered cellulose areas, leading to the release of crystalline domains, is compatible with the observed morphology. These findings demonstrate the successful production of rod-shaped CNCs from pigeon pea husk, highlighting the effectiveness of the extraction process in generating nanoscale cellulose structures [44].

3.2.2 SEM

SEM micrographs of pigeon pea husk-derived cellulose nanocrystals (CNCs) (Fig. 1b) revealed a rod-like morphology arranged in a densely interconnected network of rods and branches. This clustering can be ascribed to intermolecular hydrogen bonding and the elevated surface energy of cellulose nanocrystals. Comparable morphological characteristics have been documented for CNCs extracted from passion fruit biomass and cucumber peel [11, 45]. Dimensional analysis has been implemented by measuring more than 150 nanocrystals from the micrograph obtained by SEM. The CNCs were found to have a length of 200–350 nm and widths of 25–35 nm, with average values of 335 ± 12.91 nm and 28.80 ± 2.67 nm, respectively. The calculated aspect ratio of 11.63 confirms the elongated morphology of the isolated CNCs.

The dimensions of CNC depend on the cellulose source and processing conditions such as acid concentration, cellulose to acid ratio, temperature and time of hydrolysis. Hydrolysis conditions affect the extent of cellulose degradation and the dimensions of the resulting nanocrystals, while the intrinsic structural organization of the biomass also contributes to morphological variation [13, 46].

The aspect ratio obtained in this study falls within the intermediate range (approximately 10–15), which has been associated with effective adsorption at oil–water interfaces and the formation of compact interfacial layers with reduced particle entanglement compared with highly elongated nanocrystals [13, 47, 48]. The rod-like morphology and intermediate aspect ratio (11.63) of pigeon pea husk-derived CNCs may warrant further investigation for potential pharmaceutical applications. Future studies could explore their suitability as pharmaceutical excipients or drug-delivery carriers by evaluating drug-loading capacity, release behaviour, biocompatibility, and toxicity.

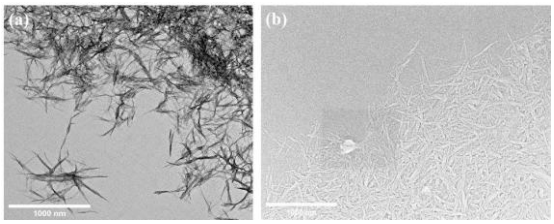


Figure 1. TEM (a) and SEM (b) images of CNCs.

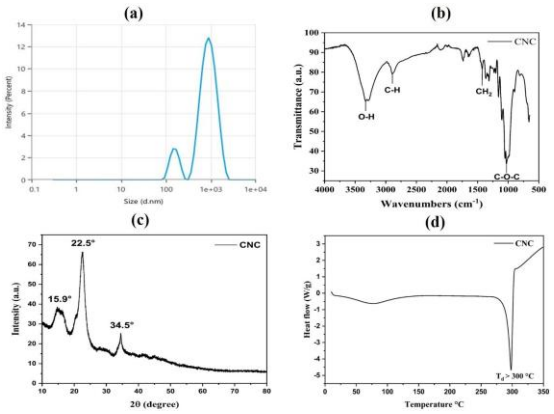


Figure 2. (a) Size distribution by intensity b) FTIR spectra (c) XRD pattern and **(b)** DSC thermogram of CNC.

3.3 Particle Size and zeta potential measurement

The zeta potential and particle size distribution of cellulose nanocrystals (CNCs) isolated from pigeon pea husk were evaluated to assess their surface charge characteristics and colloidal behaviour in aqueous suspension. The CNC suspension exhibited a zeta potential of −43.21 ± 2.34 mV, indicating a highly negative surface charge and substantial electrostatic repulsion between dispersed particles. Zeta potential values with a magnitude greater than approximately 30 mV are commonly associated with improved electrostatic stabilization in aqueous colloidal systems [49]. The high negative zeta potential observed in the present study may be attributed to the introduction of negatively charged sulfate ester groups ($–OSO_3^-$) onto the cellulose surface during sulfuric acid hydrolysis [50, 51]. These surface charges can reduce particle aggregation by increasing electrostatic repulsion between CNCs [52, 53]. However, actual suspension stability also depends on factors such as ionic strength, concentration, and storage conditions.

The hydrodynamic particle size distribution of the CNC suspension, presented in Fig. 2(a), showed an intensity-weighted mean diameter of 288.08 ± 9.07 nm and a polydispersity index (PDI) of 0.451. The measured hydrodynamic diameter reflects the apparent size of dispersed particles in the aqueous medium, including the influence of their anisotropic rod-like morphology, hydration, and possible aggregation. The PDI indicates a relatively broad particle size distribution, suggesting heterogeneity within the suspension. The presence of a tail at larger particle sizes may indicate the occurrence of some particle aggregation.

The relatively high negative zeta potential, together with the measured hydrodynamic diameter, suggests that the CNC suspension possesses favourable electrostatic characteristics for dispersion in aqueous media. Sulfuric acid hydrolysis facilitates the removal of less-ordered cellulose regions, while subsequent probe ultrasonication can help separate aggregated particles and improve dispersion. Nevertheless, some aggregation may persist because of the strong intermolecular hydrogen bonding between cellulose surfaces and the inherent tendency of nanocellulose particles to associate [54]. Although DLS provides a convenient means of assessing hydrodynamic size distribution and dispersion behaviour, its measurements should be interpreted alongside microscopy because the technique estimates an equivalent hydrodynamic diameter and does not directly measure the length and width of rod-shaped CNCs [55, 56].

3.4 FTIR

The FTIR spectrum of pigeon pea husk-derived cellulose nanocrystals (CNCs) (Fig. 2b) exhibited characteristic absorption bands at 3331, 2897, 1635, 1425, 1159, 1032, and 897 cm^{-1}. The broad band at 3331 cm^{-1} corresponded to O–H stretching vibrations, while the band at 2897 cm^{-1} was attributed to C–H stretching of aliphatic groups. The absorption band at 1635 cm^{-1} was associated with the bending vibration of absorbed moisture, reflecting the hydrophilic nature of CNCs. The band at 1425 cm^{-1} was attributed to CH_2 bending vibrations associated with cellulose structure. The bands at 1159 and 1032 cm^{-1} corresponded to C–O–C stretching of β-(1→4)-glycosidic linkages and skeletal vibrations of the cellulose pyranose ring, respectively. The band at 897 cm^{-1} was characteristic of β-glycosidic linkages in cellulose. The absence of distinct bands associated with lignin and hemicellulose, particularly carbonyl and related C–O vibrations, supported the effective removal of non-cellulosic constituents. The retention of characteristic cellulose bands indicated that the fundamental cellulose backbone remained largely intact following sulfuric acid hydrolysis, supporting the successful isolation of CNCs from pigeon pea husk [7, 34, 57-59].

3.5 X-Ray diffraction (XRD) analysis

The XRD pattern of cellulose nanocrystals (CNCs) isolated from pigeon pea husk is presented in Fig. 2(c). The CNCs exhibited a crystallinity index (CI) of 91.83%, indicating a highly ordered crystalline structure. The high crystallinity is due to selective hydrolysis of amorphous areas of cellulose during H_2SO_4 treatment, which preferentially cleaves β-1,4-glycosidic bonds in less-ordered domains and facilitates the release of crystalline nanodomains [60, 61]. Consequently, the resulting CNCs exhibit a greater proportion of ordered cellulose regions relative to amorphous domains. However, the

measured CI is also influenced by the cellulose source, isolation and hydrolysis conditions, and the analytical method used for crystallinity estimation [39, 62].

The high crystallinity of the obtained CNCs highlights their potential as reinforcing nanofillers in biopolymer composites. Their ordered structure may contribute to improved mechanical strength, stiffness, and rigidity when suitable interfacial interactions and dispersion are achieved within the polymer matrix. Nevertheless, these performance benefits depend on the composite formulation and processing conditions and would require experimental validation [11, 49, 55, 60].

3.6 DSC

The DSC thermogram of pigeon pea husk-derived cellulose nanocrystals (CNCs) (Fig. 2d) exhibited an initial endothermic transition between 50 and 110 °C, attributed to the evaporation of physically adsorbed and bound moisture. A prominent thermal event was observed near 300 °C, indicating a major thermal transition associated with the CNC structure. This behaviour may reflect the thermal decomposition of cellulose, influenced by its structural organization and the presence of sulfate ester groups introduced during sulfuric acid hydrolysis. The thermal response of CNCs is affected by crystallinity, particle dimensions, surface chemistry, and hydrolysis conditions. Overall, the observed thermal transitions provide insight into the thermal behaviour of the isolated CNCs and may help guide future investigations into their suitability for thermally processed biomaterial systems.

Conclusion

This study demonstrates the successful production of cellulose nanocrystals (CNCs) from pigeon pea husk through controlled sulfuric acid hydrolysis. Hydrolysis using 64 wt.% sulfuric acid at 45 °C for 30 min, followed by probe sonication, yielded 61.25% CNCs relative to the purified cellulose, with a crystallinity index of 91.83%. The CNCs exhibited a hydrodynamic diameter of 288.08 ± 9.07 nm and a zeta potential of −43.21 ± 2.34 mV, indicating favourable electrostatic characteristics for aqueous dispersion. Morphological characterization confirmed the formation of rod-shaped nanocrystals with an average length of 335 ± 12.91 nm, width of 28.80 ± 2.67 nm, and an aspect ratio of 11.63. Spectroscopic analysis supported the retention of the characteristic cellulose structure, while thermal analysis revealed a prominent thermal event around 300 °C. These findings establish pigeon pea husk as a promising renewable feedstock for CNC production. Further investigations into thermal stability, biocompatibility, and functional performance are required to assess the suitability of these CNCs for potential applications in biodegradable packaging, Pickering emulsion stabilization, and pharmaceutical systems.

Acknowledgment

The authors would like to express their sincere gratitude to the Department of Food and Nutrition & Department of Pharmaceutical Sciences, Babasaheb Bhimrao Ambedkar University, Lucknow, for providing their laboratory facilities to conduct experiments and complete this study.

Credit authorship contribution statement

Conceptualization: Neetu Singh & Alka Nanda; Methodology: Alka Nanda; Resources: Neetu Singh; Software: Alka Nanda; Supervision: Neetu Singh; Validation: Neetu Singh; Writing - original draft: Alka Nanda; Writing - review & editing: Alka Nanda

Conflict of Interest

The authors declared no potential conflict of interest with respect to the authorship and publication.

Funding source

No funding organization in the public, private, or non-profit sectors, including universities, gave a designated grant in support of this research.

Ethics approval

Not applicable. Ethical approval was not required for this study, as it did not involve human or animal subjects.

Consent to participate

Not applicable. This research did not involve human participants.

Consent for publication

All authors provide their consent for the publication of this manuscript.

Availability of data and material

The datasets generated and analyzed during the current study are available from the corresponding author on reasonable request.

Declaration of Generative AI in Scientific Writing

This is to certify that the research presented in this manuscript has been conducted solely by the authors without the assistance of generative AI tools in any stage of scientific writing, including the conception, drafting, revising, and editing of the manuscript. All analyses, interpretations, and conclusions are the original work of the authors, derived from the referenced studies and methodologies employed. No AI tools were used to generate text, images, or data interpretations for this submission.

Code availability

Not applicable. No software applications or custom codes were used in this research.

References

1. Klemm, D., et al., *Cellulose: fascinating biopolymer and sustainable raw material.* 2005. **44**(22): p. 3358-3393.
2. George, J., S.J.N. Sabapathi, science, and applications, *Cellulose nanocrystals: synthesis, functional properties, and applications.* 2015: p. 45-54.

3. Le Normand, M., R. Moriana, and M.J.C.p. Ek, *Isolation and characterization of cellulose nanocrystals from spruce bark in a biorefinery perspective.* 2014. **111**: p. 979-987.
4. Li, J., et al., *Homogeneous isolation of nanocellulose from sugarcane bagasse by high pressure homogenization.* 2012. **90**(4): p. 1609-1613.
5. Li, Y., et al., *High Yield Preparation Method of Thermally Stable Cellulose Nanofibers.* 2014. **9**(2).
6. Jiang, F. and Y.-L.J.C.p. Hsieh, *Chemically and mechanically isolated nanocellulose and their self-assembled structures.* 2013. **95**(1): p. 32-40.
7. Rhim, J.-W., J.P. Reddy, and X.J.C. Luo, *Isolation of cellulose nanocrystals from onion skin and their utilization for the preparation of agar-based bio-nanocomposites films.* 2015. **22**(1): p. 407-420.
8. Henriksson, M., et al., *An environmentally friendly method for enzyme-assisted preparation of microfibrillated cellulose (MFC) nanofibers.* 2007. **43**(8): p. 3434-3441.
9. Alemdar, A. and M.J.B.t. Sain, *Isolation and characterization of nanofibers from agricultural residues–Wheat straw and soy hulls.* 2008. **99**(6): p. 1664-1671.
10. Chen WenShuai, C.W., et al., *Individualization of cellulose nanofibers from wood using high-intensity ultrasonication combined with chemical pretreatments.* 2011.
11. Prasanna, N.S. and J.J.C.P. Mitra, *Isolation and characterization of cellulose nanocrystals from Cucumis sativus peels.* 2020. **247**: p. 116706.
12. Lu, P. and Y.-L.J.C.P. Hsieh, *Preparation and characterization of cellulose nanocrystals from rice straw.* 2012. **87**(1): p. 564-573.
13. Oun, A.A. and J.-W.J.C.p. Rhim, *Isolation of cellulose nanocrystals from grain straws and their use for the preparation of carboxymethyl cellulose-based nanocomposite films.* 2016. **150**: p. 187-200.
14. Kumar, A.K., S.J.B. Sharma, and bioprocessing, *Recent updates on different methods of pretreatment of lignocellulosic feedstocks: a review.* 2017. **4**(1): p. 7.
15. Bian, H., et al., *Value-added utilization of wheat straw: from cellulose and cellulose nanofiber to all-cellulose nanocomposite film.* 2022. **12**(5): p. 475.
16. Borrega, M., et al., *Utilizing and valorizing oat and barley straw as an alternative source of lignocellulosic fibers.* 2022. **15**(21): p. 7826.
17. Kumari, P., et al., *Valorization of Barley Straw and Husk: Valorization Methods and Packaging Applications*, in *Agro-Wastes for Packaging Applications*. 2024, CRC Press. p. 66-82.
18. Hafid, H.S., et al., *Enhanced crystallinity and thermal properties of cellulose from rice husk using acid hydrolysis treatment.* 2021. **260**: p. 117789.
19. Vu, A.N., et al., *Cellulose nanocrystals extracted from rice husk using the formic/peroxyformic acid process: isolation and structural characterization.* 2024. **14**(3): p. 2048-2060.
20. Ning, P., et al., *Recent advances in the valorization of plant biomass.* 2021. **14**(1): p. 102.
21. Reddy, N. and Y.J.B.T. Yang, *Natural cellulose fibers from soybean straw.* 2009. **100**(14): p. 3593-3598.
22. Velásquez-Castillo, L.E., et al., *Physical properties of gelatin-based hydrogels incorporated with soybean straw nanocellulose obtained by enzymatic hydrolysis.* 2025. **14**(13): p. 2269.
23. Jeevarathinam, G. and V. Chelladurai, *Pigeon pea*, in *Pulses: Processing and Product Development*. 2020, Springer. p. 275-296.
24. Pal, D., et al., *Biological activities and medicinal properties of Cajanus cajan (L) Millsp.* 2011. **2**(4): p. 207-214.
25. Sarkar, S., et al., *Pigeon pea (Cajanus cajan) an important food legume in Indian scenario-A review.* 2020. **43**(5): p. 601-610.
26. Sethi, S., et al., *Development and quality evaluation of quick cooking dhal—A convenience product.* 2014. **51**(3): p. 595-600.
27. Susmitha, D., et al., *Calcium-Rich pigeonpea seed coat: a potential byproduct for food and pharmaceutical industries.* 2022. **14**(9): p. 4918.
28. Abe, K., S. Iwamoto, and H.J.B. Yano, *Obtaining cellulose nanofibers with a uniform width of 15 nm from wood.* 2007. **8**(10): p. 3276-3278.
29. Abe, K. and H.J.C. Yano, *Comparison of the characteristics of cellulose microfibril aggregates isolated from fiber and parenchyma cells of Moso bamboo (Phyllostachys pubescens).* 2010. **17**: p. 271-277.
30. Dong, S. and M.J.J.o.t.A.C.S. Roman, *Fluorescently labeled cellulose nanocrystals for bioimaging applications.* 2007. **129**(45): p. 13810-13811.

31. Roman, M. and D.G.J.L. Gray, *Parabolic focal conics in self-assembled solid films of cellulose nanocrystals.* 2005. **21**(12): p. 5555-5561.
32. Jiang, F. and Y.-L.J.C.P. Hsieh, *Cellulose nanocrystal isolation from tomato peels and assembled nanofibers.* 2015. **122**: p. 60-68.
33. Makhado, E., et al., *Comparative extraction and characterisation of cellulose nanostructures from sawdust and maize stalk biomass.* 2025: p. 147842.
34. Singh, S., et al., *Insights into thermal degradation kinetics and liquid crystalline behavior of cellulose nanocrystals from the waste of Cajanus cajan (pigeon pea).* 2023. **242**: p. 124507.
35. Nanda, A. and N.J.A.F.S.J. Singh, *Preparation and antimicrobial activity of corn cob and coir reinforced biodegradable starch biocomposite films for food packaging application.* 2022. **21**(7): p. 53-66.
36. Nanda, A., et al., *Revolution of nanotechnology in food packaging: Harnessing electrospun zein nanofibers for improved preservation-A review.* 2024. **260**: p. 129416.
37. Pandey, G., et al., *Multilayered nanofibrous scaffold of Polyvinyl alcohol/gelatin/poly (lactic-co-glycolic acid) enriched with hemostatic/antibacterial agents for rapid acute hemostatic wound healing.* 2023. **638**: p. 122918.
38. Shyam Kumar, R., et al., *A new natural cellulosic pigeon pea (Cajanus cajan) pod fiber characterization for bio-degradable polymeric composites.* 2021. **18**(9): p. 1285-1295.
39. Rasheed, H.A., et al., *Isolation, characterization and response surface method optimization of cellulose from hybridized agricultural wastes.* 2024. **14**(1): p. 14310.
40. Bondeson, D., A. Mathew, and K.J.C. Oksman, *Optimization of the isolation of nanocrystals from microcrystalline cellulose by acid hydrolysis.* 2006. **13**(2): p. 171-180.
41. Hu, S., et al., *Holistic rice straw nanocellulose and hemicelluloses/lignin composite films.* 2016. **4**(3): p. 728-737.
42. Coelho, C.C., et al., *Cellulose nanocrystals from grape pomace: Production, properties and cytotoxicity assessment.* 2018. **192**: p. 327-336.
43. Mazlita, Y., et al., *Preparation of cellulose nanocrystals bio-polymer from agro-industrial wastes: Separation and characterization.* 2016. **24**(9): p. 719-728.
44. Kaushik, M., et al., *Transmission electron microscopy for the characterization of cellulose nanocrystals*. 2015: IntechOpen.
45. Wijaya, C.J., et al., *Cellulose nanocrystals from passion fruit peels waste as antibiotic drug carrier.* 2017. **175**: p. 370-376.
46. Morais, J.P.S., et al., *Extraction and characterization of nanocellulose structures from raw cotton linter.* 2013. **91**(1): p. 229-235.
47. Korolovych, V.F., et al., *Cellulose nanocrystals with different morphologies and chiral properties.* 2018. **145**: p. 334-347.
48. Kalashnikova, I., et al., *Cellulosic nanorods of various aspect ratios for oil in water Pickering emulsions.* 2013. **9**(3): p. 952-959.
49. Naduparambath, S., et al., *Isolation and characterisation of cellulose nanocrystals from sago seed shells.* 2018. **180**: p. 13-20.
50. Feng, Y., S.R. Kilker, and Y. Lee, *Surface charge (zeta-potential) of nanoencapsulated food ingredients*, in *Characterization of nanoencapsulated food ingredients*. 2020, Elsevier. p. 213-241.
51. Németh, Z., et al., *Quality by design-driven zeta potential optimisation study of liposomes with charge imparting membrane additives.* 2022. **14**(9): p. 1798.
52. El Achaby, M., et al., *Production of cellulose nanocrystals from vine shoots and their use for the development of nanocomposite materials.* 2018. **117**: p. 592-600.
53. Pirich, C.L., et al., *Influence of mechanical pretreatment to isolate cellulose nanocrystals by sulfuric acid hydrolysis.* 2019. **130**: p. 622-626.
54. Hemmati, F., et al., *Synthesis and characterization of cellulose nanocrystals derived from walnut shell agricultural residues.* 2018. **120**: p. 1216-1224.
55. Melikoğlu, A.Y., S.E. Bilek, and S.J.C.p. Cesur, *Optimum alkaline treatment parameters for the extraction of cellulose and production of cellulose nanocrystals from apple pomace.* 2019. **215**: p. 330-337.
56. Boluk, Y. and C.J.J.o.n.r. Danumah, *Analysis of cellulose nanocrystal rod lengths by dynamic light scattering and electron microscopy.* 2014. **16**(1): p. 2174.
57. Khenblouche, A., et al., *Extraction and characterization of cellulose microfibers from Retama raetam stems.* 2019. **29**: p. e2019011.
58. Tibolla, H., et al., *Cellulose nanofibers produced from banana peel by chemical and mechanical treatments:*

characterization and cytotoxicity assessment. 2018. **75**: p. 192-201.
59. Bosenbecker, M.W., et al., *Isolation of cellulose nanocrystals from Bambusa vulgaris pulp via physio-chemical approach.* 2024. **14**(13): p. 14153-14162.
60. Collazo-Bigliardi, S., R. Ortega-Toro, and A.C.J.C.p. Boix, *Isolation and characterisation of microcrystalline cellulose and cellulose nanocrystals from coffee husk and comparative study with rice husk.* 2018. **191**: p. 205-215.
61. Doh, H., M.H. Lee, and W.S.J.F.h. Whiteside, *Physicochemical characteristics of cellulose nanocrystals isolated from seaweed biomass.* 2020. **102**: p. 105542.
62. Vieyra, H., et al., *Optimized monitoring of production of cellulose nanowhiskers from Opuntia ficus-indica (nopal cactus).* 2015. **2015**(1): p. 871345.